Available online at www.sciencedirect.com
SCIENCE DIRECT
Catalysis Today 116 (2006) 400–407
CATALYSIS TODAY
www.elsevier.com/locate/cattod

Water–gas shift reaction over sulfided molybdenum catalysts supported on TiO_2–ZrO_2 mixed oxides Support characterization and catalytic activity

M. Laniecki *, M. Ignacik

Faculty of Chemistry, A. Mickiewicz University, ul. Grunwaldzka 6, 60-780 Poznań, Poland

Available online 10 July 2006

Abstract

Supported sulfided molybdenum and nickel–molybdenum catalysts were applied in the water–gas shift (WGS) reaction with sulfided feed. TiO_2, ZrO_2 and binary systems of TiO_2–ZrO_2, in which composition was changed in 10 wt.% intervals, were used as the supports for sulfided Mo and Ni–Mo catalysts. The concentration of Mo (8 wt.%) and Ni (3 wt.%) was the same in all studied catalysts. Supports and selected catalysts were characterized with XRD, BET, TPR (H_2), TPD of ammonia, FTIR and NO adsorption measurements. The comparison of pure TiO_2 or ZrO_2 with TiO_2–ZrO_2 systems shows that introduction of the second component always resulted in almost duplication of the surface area of the supports. No simple relationship between surface area and catalytic activity was found. The choice of the support with appropriate ratio of surface acid–base sites, high dispersion of supported Ni–Mo–S surface species as well as much easier reductivity of Mo^{6+} ions in the presence of nickel ions can lead towards high activity in the WGS reaction with sulfided feed. The highest activity was obtained for Ni–Mo–S catalysts supported on TiO_2 (40)–ZrO_2 (60).

Keywords: Hydrogen; Water–gas shift; Molybdenum sulfide; Ni–Mo–S; TiO_2–ZrO_2 support

1. Introduction

The most important global problems of the 21st century are primary energy and global warming. According to the optimistic prediction of the Organization for Economic Collaboration and Development and major oil companies, estimated minable reserves of oil and natural gas to be depleted in around 45 and 65 years, respectively. The oil supply will fall dawn below the demand level around 2015 (''Roll Over Point''), pushing the oil prices to a drastically high level. Resolution of these problems require intensive search in development of new energy systems.

Due to the unique properties, hydrogen is forecast to become a major source of energy in the next decades. However, future use of hydrogen by consumers is very much limited by the methods of its generation. At the moment steam methane reforming (SMR) is the largest and the cheapest method of hydrogen production [1]. Future world energy requirements will need to use renewable sources of H_2 in order to reduce pollution. Among different methods of future hydrogen generation the use of biomass attracts much attention [2]. Biomass pyrolysis or biomass steam reforming can be applied in hydrogen production, however, carbon monoxide formation always accompany this processes. In all these cases, catalytic water–gas shift (WGS) reaction is proposed to solve the problem of CO removal. Moreover, in this reaction additional amounts of hydrogen can be produced.

Water–gas shift reaction is the catalytic reaction well known since more than a century and is very important step in industrial production of hydrogen. Both low-temperature (Cu–Zn–O) and high-temperature (Fe–Cr–O) catalysts used in this process are very sensitive towards sulfur contamination of the feed [3]. Due to constant increase of the sulfur containing compounds in the WGS feed, what is closely related with the lowering of the substrates quality (e.g. also gases evolved during biomass pyrolysis), the new class of catalysts based mainly on molybdenum sulfides were introduced into the market. These catalysts allow to perform this WGS process,

* Corresponding author. Fax: +48 61 8291339.
E-mail address: laniecki@amu.edu.pl (M. Laniecki).

0920-5861/$ – see front matter © 2006 Elsevier B.V. All rights reserved.
doi:10.1016/j.cattod.2006.05.080

known also as ''Sour Gas Shift'' [4] with feeds containing even large quantities of hydrogen sulfide. However, some of these catalysts undergo rather rapid deactivation in the presence of olefins and oxygenates in the feed. In order to expand their lifetime, as well as to improve their catalytic activity many laboratories look for new methods of preparation of these catalysts as well as the use of new supports for the WGS applications. So far, only few papers discussed the application of supported molybdenum sulfides in the WGS reaction [5–9] and practically no systematic studies of the influence of the applied oxide support on catalytic activity were performed. Our earlier studies [10–12] showed that wide pore Y-zeolites can be good supports for Ni–Mo–S catalysts in the WGS reaction.

It is well known that TiO_2 and ZrO_2, as well as the binary systems of these oxides, can serve not only as good catalysts but also as the excellent supports for Co–Mo or Ni–Mo sulfides applied in hydrotreatment reactions (HDS, HDN, HYD). Due to the specific acid–base surface properties of TiO_2, ZrO_2 and their mixtures [13–15], it was interesting to apply these supports for preparation of Ni–Mo–S catalysts operating with sulfided feed in water–gas shift reaction and to check their catalytic performance. Therefore, the purpose of the present work was to examine the surface properties of prepared binary TiO_2–ZrO_2 systems on catalytic activity in the WGS reaction. This paper describes the family of completely sulfur-tolerant WGS catalysts based on nickel and molybdenum supported on mixed systems of TiO_2–ZrO_2.

2. Experimental

2.1. Preparation of the supports

TiO_2 and ZrO_2 were prepared by hydrolysis from $TiCl_4$ and $Zr(NO_3)_4$, respectively, and final precipitation with ammonia (final pH 9). In the case of titania 0.1 mol of $TiCl_4$ was added dropwise to 1 dm^3 of distilled water kept at 345 K. Pure zirconia was obtained in similar manner applying 0.06 mol of $Zr(NO_3)_4$. In both cases final addition of ammonia completed precipitation. The binary systems TiO_2–ZrO_2, in which the weight ratio of TiO_2 to ZrO_2 was changed every 10 wt.% were obtained in three steps. In the first one, an appropriate amount of $TiCl_4$ was introduced into 1 dm^3 of water kept at 345 K and partially formed, hydrated $Ti(OH)_4$ was dissolved with HCl until clear solution was obtained. In the second step, the calculated amount of crystalline $Zr(NO_3)_4$ was added to the solution of $TiCl_4$ while vigorously stirring. The dropwise addition (third step) of 25 vol.% solution of ammonia till pH 9 completed the precipitation of the binary systems. Hydrated gels of TiO_2, ZrO_2 and TiO_2–ZrO_2 systems, after removal of Cl^- or NO_3^- ions, were dried at 375 K and calcined at 675 K for 2 h.

2.2. Preparation of catalysts

Catalysts containing 8 wt.% of Mo were prepared by impregnation of the supports with ammonia–water solution of H_2MoO_4, applying incipient wetness method. After drying at 375 K (24 h), the oxidized forms of catalysts were obtained after calcination at 675 K (2 h). Nickel containing catalysts (3 wt.%) were obtained similarly. For impregnations, the water solution of nickel nitrate was applied. In the case Ni–Mo catalysts, molybdenum was deposited first and after procedures described above, and next impregnation with $Ni(NO_3)_2$ was performed. After drying and calcination catalysts in oxidized forms were obtained. All samples applied in catalytic tests were sulfided in situ in stream of hydrogen containing 10 vol.% of H_2S at 675 K. All other samples, after sulfidation at 675 K were cooled down in stream of the sulfidation mixture and flushed with argon at room temperature.

2.3. Catalytic activity

Catalysts weighing 0.5 g (grains 0.5–1.0 mm) were placed in the fixed-bed reactor operating under atmospheric pressure and next sulfided in H_2S/H_2 flow at 675 K. After 2 h sulfidation, the temperature was lowered to 625 K and the WGS reaction was initiated. The reaction mixture was composed from 49 vol.% of H_2, 49 vol.% of CO and 2 vol.% of H_2S. In majority of experiments the H_2:CO ratio was one. Analysis of gases was performed with GC (Varian 3800) and automatic gas sampling valve.

2.4. Supports characterization

Samples were characterized with XRD (modified TUR-62 spectrometer), thermogravimetric analysis (Setsys TG-DSC from Setaram), nitrogen adsorption at 78 K (ASAP-2010), NO adsorption by pulse technique at 295 K, TPD of ammonia and TPR (Chemisorb 2705) and FTIR measurements (Vector-22 from Bruker) with pyridine as probe molecule. The details of the techniques applied for support characterization can be found in another paper [8].

3. Results and discussion

The activity of the WGS catalysts operating with ''sour gas'' strongly depends on the composition of metals sulfides of the groups VI and VIII (other than Cr and Fe) supported on different ''white'' oxides or their mixtures. However, the use of appropriate support can strongly influence the activity and the lifetime of the applied catalysts. Therefore, the results presented in this paper are focused on characteristics of the applied support and catalytic activity in the WGS reaction.

3.1. Supports

TiO_2, ZrO_2 and differing in composition TiO_2–ZrO_2 mixed oxides were applied in this paper as the supports. For the applied supports the following notation is applied: first number indicate concentration of TiO_2 in wt.%, whereas the second, concentration of ZrO_2.

Simultaneous registration of TG, DTG, TA and DTA during thermogravimetric analysis of the hydrated supports allowed to establish that calcination temperature at 675 K which is

Table 1
Characteristic of the supports

Support	Mass loss 675–1175 K (%)	DTA exothermic effect (K)	BET surface area ($m^2\ g^{-1}$)	Pore volume ($cm^3\ g^{-1}$)	Average pore diameter (nm)	Lewis acidity (a.u.)	TPD maxima of NH_3 (K)
TiO_2	0.69	Not observed	168	0.33	6.0	492	600; 800; 1000
90Ti–10Zr	0.50	Not observed	256	0.38	5.7	798	
80Ti–20Zr	0.78	Not observed	276	0.40	5.6	816	600; 800; 1000
70Ti–30Zr	1.17	1035	278	0.41	5.3	820	
60Ti–40Zr	1.02	1015	279	0.44	5.1	825	580; 800–900
50Ti–50Zr	1.17	1005	280	0.45	5.0	836	
40Ti–60Zr	1.30	1005	269	0.39	4.9	580	580; 900
30Ti–70Zr	1.34	975	267	0.34	4.7	506	
20Ti–80Zr	1.46	945	264	0.30	4.5	425	580; 900
10Ti–90Zr	1.70	835	247	0.25	4.2	396	
ZrO_2	1.81	725	167	0.19	3.8	242	600; 950

sufficient enough to stabilize the supports and is still far from the sintering effects. Above this temperature only slight decrease of weight loss up to 1175 K was observed for all samples in dynamic conditions (heating rate 15 K min^{-1}). It was the highest for ZrO_2 (compare data in Table 1). The increasing amount of ZrO_2 in the supports resulted in higher concentration of surface hydroxyl groups and their relatively stronger bonding. The analysis of thermal effects (see Fig. 1, TA curves) up to 675 K leads to conclusions that depending on the composition of hydrated support, the endothermic effects are related with water evolution. This was confirmed by mass spectroscopic measurements. For TiO_2 only one strong effect was observed close to 380 K, whereas with increasing concentration of ZrO_2 the second endothermic effect at 475 K appeared. This indicates the two-step mechanism during dehydratation of hydrated ZrO_2 or samples containing this oxide, in which majority of weakly bonded water is removed at about 375 K. The exothermic effects related with phase transformations of the prepared supports appear at temperatures higher than 700 K (see data collected in Table 1). The exothermic peak on TA curve of ZrO_2 at 725 K indicates that phase transformation from amorphous to monoclinic occurs [16]. In the binary systems very intense exothermic peak at 1035 K started to appear for samples containing more than 30 wt.% of ZrO_2. The increase of ZrO_2 concentration resulted in the shift of this effect towards lower temperatures. With maximum at 1005 K for 50Ti–50Zr sample formation of zirconium titanate ($ZrTiO_4$) can be observed. Formation of this phase has been confirmed by the X-ray diffraction experiments in which the appearance of the very intense reflex at 30.6 (2Θ) (for samples calcined at 1075 K) is characteristic for zirconium titanate phase presence [14,17]. At lower calcination temperatures this effect was not observed. Higher concentration of ZrO_2 in synthesized supports shifted exothermic peak on TA curves towards lower temperatures. Relatively low temperature of this transformation can be explained by the strong influence of preparation conditions (pH, initial concentration of the zirconium salt and applied precursor).

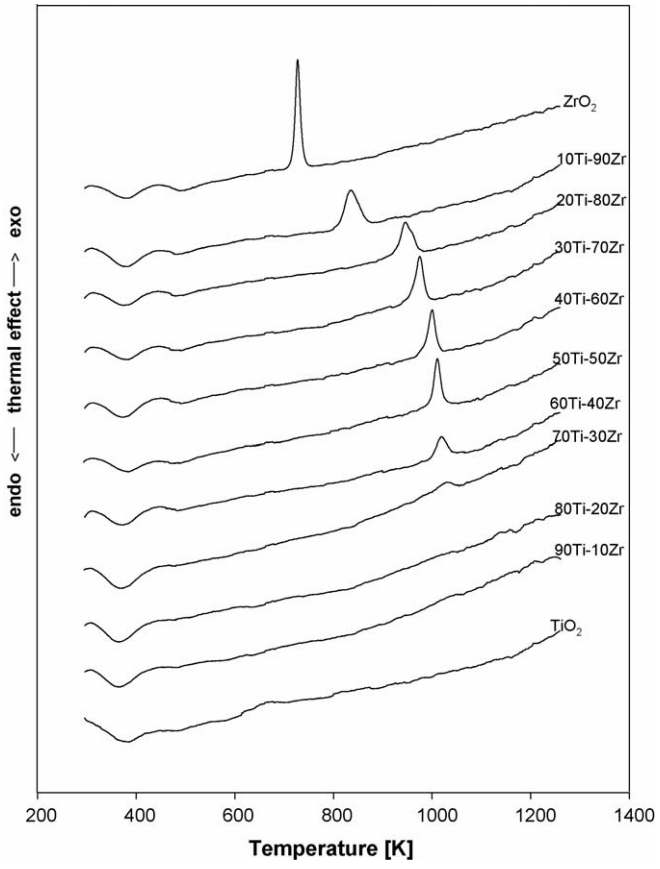

Fig. 1. Differential thermal analysis (DTA) profiles.

XRD diffraction patterns of the samples calcined at 675 K showed that only pure TiO_2 and ZrO_2 indicate characteristic reflexes of anatase [13,18] and poorly crystallized monoclinic phase of zirconia [19,20], respectively. XRD measurements of all other supports calcined at the same temperature showed lack of crystallinity and practically amorphous character. However, samples with higher concentration of TiO_2 (90Ti–10Zr and 80Ti–20Zr) after calcination at 675 K showed weak reflexes originating from anatase. Further increase of ZrO_2 concentration in this binary system resulted in completely amorphous samples. Calcination of all samples at 1075 K resulted in formation of crystalline structures (from rutile-TiO_2, to well defined monoclinic ZrO_2). These samples, however, did not serve in our further studies as the supports, due to the significant decrease of surface area caused by sintering.

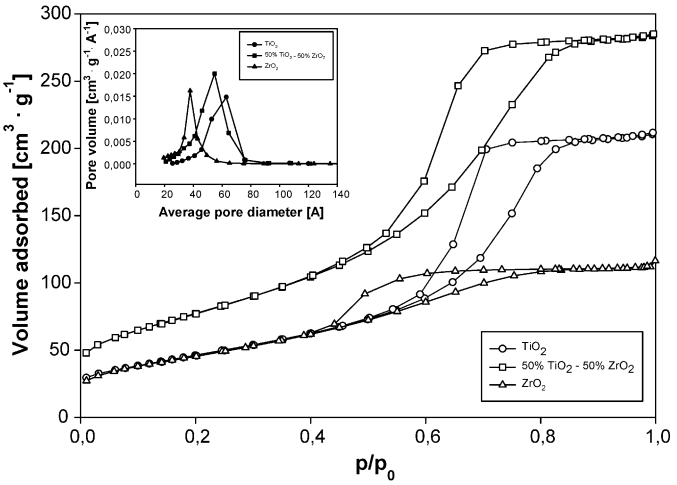

Fig. 2. Adsorption–desorption isotherms of N_2 at 77 K and pore size distribution of selected supports.

The amorphous character of the majority of binary systems caused the significant increase of surface area of the studied supports. Surface area of the supports calcined at 675 K, based on the measurements of adsorption of nitrogen at 77 K, are shown in Table 1, whereas typical shapes of the adsorption–desorption isotherms for pure titania, zirconia and 50Ti–50Zr sample are illustrated on Fig. 2. The shape of adsorption–desorption isotherms indicate that independently of the composition all samples indicate the mesoporous character. This is confirmed by the presence and position of characteristic hysteresis loops for all studied supports. The position of hysteresis loop of ZrO_2 between 0.4 and 0.8 p/p and characteristic shape (H4) is indicative for the presence of rather uniform slit pores. This is well documented on the pore size distribution curve (see insert on Fig. 2). In contrast, for titania the shape of hysteresis loop (H2) indicate less uniform distribution of mesopores. As previously, it finds the reflection in the pore size distribution curve (insert in Fig. 2). The shape and the positions of isotherms for the binary systems are exemplified on Fig. 2 for the 50Ti–50Zr sample. All other compositions of these supports showed almost identical values of adsorbed nitrogen and very similar shape of isotherms. The consequence of such behaviour is reflected in the values of BET surface area of the studied supports (see Table 1).

The almost identical and relatively high values of surface area of TiO_2 and ZrO_2 were always almost doubled after introduction of the second component into one of these oxides. High values of surface area of the separate oxides, especially for zirconia, result from the preparation procedure and applied compounds. Application of organic precursors for synthesis either of titania or zirconia leads usually to much lower values of surface area [8,20], usually close to 50 $m^2\ g^{-1}$. On the other hand the binary systems reach the maximum of surface area (280 $m^2\ g^{-1}$) for supports containing 50 wt.% of each component. Such increase of surface area for binary system is the result of lower degree of crystallization. This tendency was confirmed by other authors who applied different compounds of Ti and Zr [14,21,22]. Pore volume of the studied systems indicate, depending on the composition, shape of volcano curve with the lovest values for pure titania and zirconia. Pore size distribution calculated by BJH method shows constant decrease of pore size dimensions with decreasing content of TiO_2 and reaching the lowest value for ZrO_2.

Surface acidity of the applied supports was studied both in infrared experiments with adsorbed pyridine and TPD of ammonia. The FTIR experiments with pyridine as the probe molecule indicated only presence of the Lewis acid sites (band at 1440 cm^{-1}). Data presented in Table 1 show changes in relative Lewis acid sites concentration (after pyridine desorption at 375 K) and their distribution expressed there as temperature maxima on TPD curves. Fig. 3 shows characteristic TPD

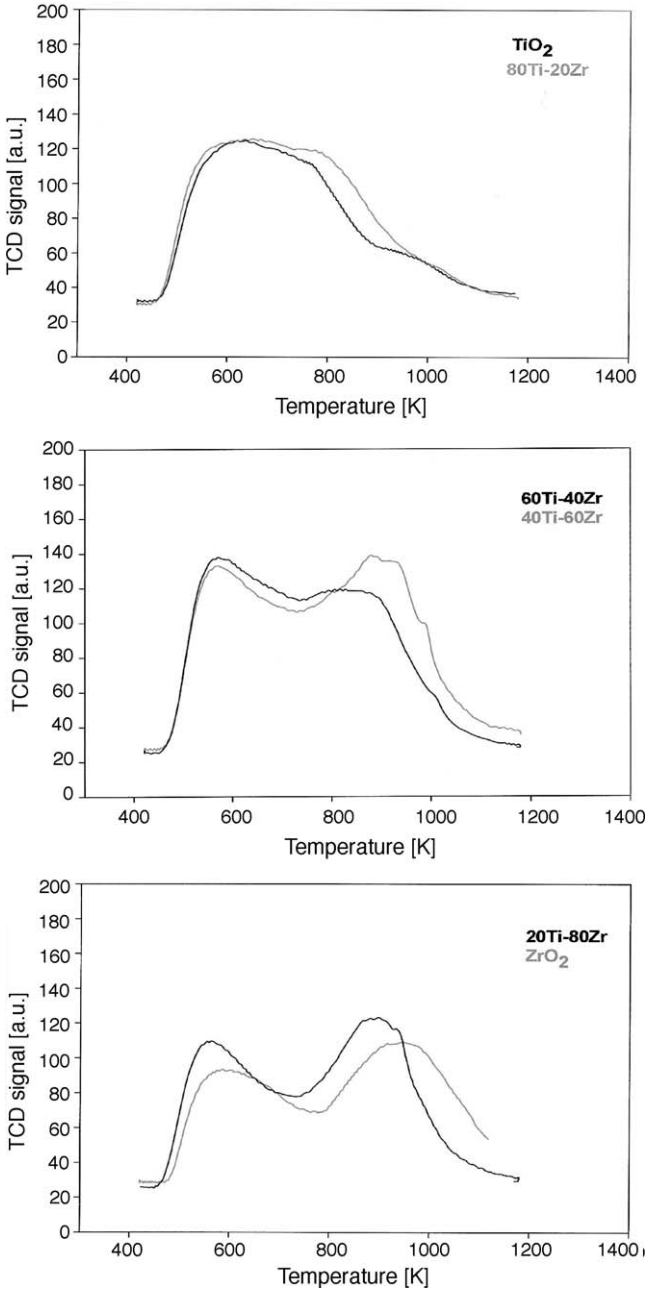

Fig. 3. Temperature programmed desorption (TPD) curves of ammonia for selected supports.

profiles obtained for selected samples. Similarly to the earlier studies performed in other laboratories [23–25] also in our case the overall acidity of these supports increased with higher content of ZrO_2 in the mixture. Data presented in Table 1 indicate that the highest concentration of weak surface acid sites takes place for supports composed of 50% of TiO_2 and ZrO_2. The infrared experiments were confirmed by the temperature programmed desorption of ammonia. TPD profiles (see examples on Fig. 3) for TiO_2 indicate presence of at least three different acid sites at ~600, 800 and 1000 K and only two for pure ZrO_2. For TiO_2 these sites are rather weak, what is demonstrated by the presence of one broad desorption peak of ammonia between 600 and 800 K with weak shoulder around 1000 K. Higher content of ZrO_2 in the support generate at least one new stronger site (desorption peak at ~900 K) and increase in the population of the weaker one (desorption peak at ~580 K). In the case of ZrO_2 two acid centers can be observed, however, the desorption maxima of NH_3 show that their character is completely different than in the case of TiO_2. All obtained TPD results are in good agreement with those received in FTIR measurements.

3.2. Catalytic activity

Catalytic activity of the supported Mo and Ni–Mo sulfides was tested in the water–gas shift reaction at 625 K, and CO:H_2O ratio in majority of experiments was equal to 1. Each catalyst prior to the catalytic reaction was sulfided at 675 K. Fig. 4 shows the results of WGS catalytic activity expressed as the pseudo-first-order reaction rate constant of the selected catalysts *versus* time of reaction. The results presented for TiO_2, ZrO_2 and the most active catalyst based on 40Ti–60Zr support indicates that the best performance was found for catalysts based on supported Ni–Mo–S species. In contrast, supported molybdenum or nickel sulfide separately shows much lower activity. Pure supports after similar procedure of sulfidation indicated lack of activity. In majority of the WGS experiments the stabilization of catalytic activity was observed after 2 h of reaction.

The influence of the applied support on catalytic activity, both for sulfided Mo, Ni and Ni–Mo catalysts, is shown in Fig. 5. Activity usually slightly increased during the reaction but after 2 h was practically stabilized. The obtained results show that the influence of applied supports, especially those of mixed composition, has a significant importance on catalytic performance in the WGS reaction. As it was shown earlier, the best catalysts were supported on supports composed from 40 wt.% of TiO_2 and 60 wt.% ZrO_2 and containing 8 wt.% of Mo and 3 wt.% of Ni.

Considering differing factors influencing activity in the WGS process one can conclude that, among others, specific surface area is one of these factors. Comparison of present results with those obtained earlier for TiO_2 and ZrO_2 supports (same loadings of Mo and Ni) but with lower values of BET surface area [8] shows that higher surface area causes better dispersion and catalytic activity. In general, the increased surface area of the applied supports is responsible for better

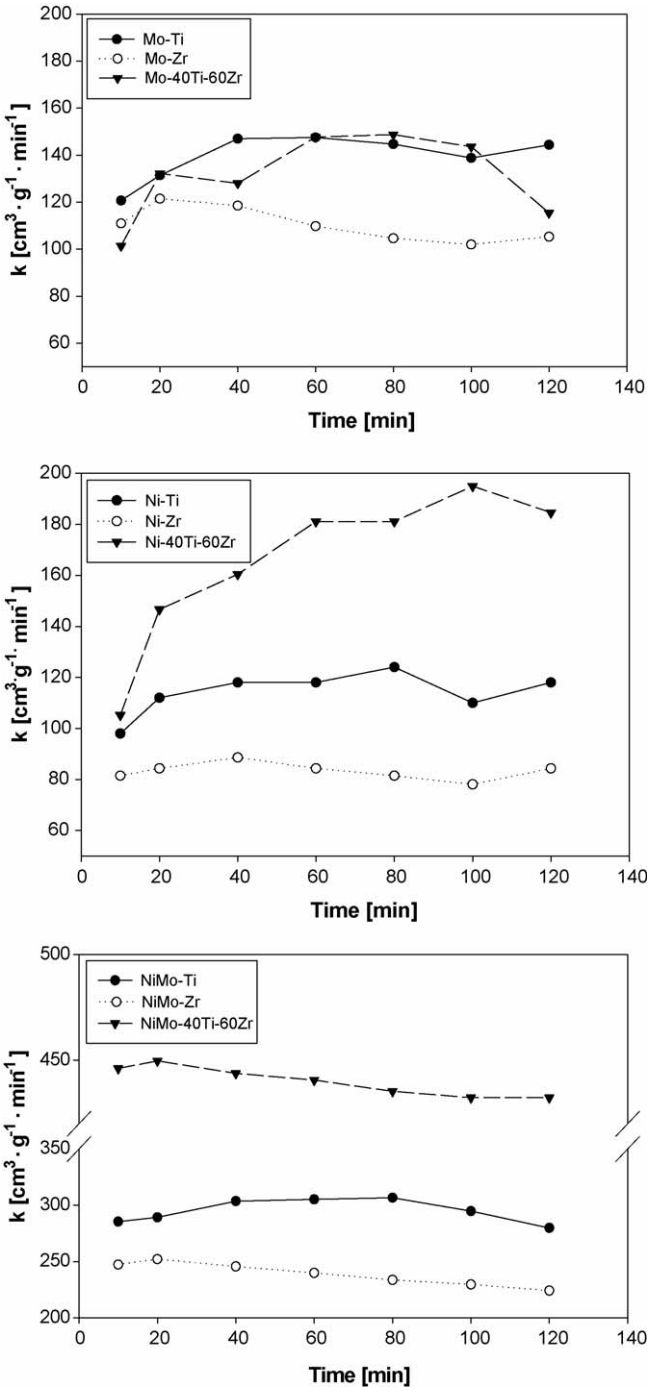

Fig. 4. Catalytic activity in the WGS reaction of catalysts supported on 40 wt.%.TiO_2–60 wt.% ZrO_2.

dispersion of sulfided structures (Table 2), however, this role within the Ti–Zr mixed oxide supports is rather weak. It is known from literature [26–28] that presence and distribution of surface hydroxyl groups on TiO_2 or ZrO_2 play a significant role during MoO_3 monolayer formation, and in consequence further dispersion of molybdenum sulfides. Data presented on Fig. 5 show that both in the case of supported molybdenum or nickel sulfides the activity is rather low in comparison with Ni–Mo–S catalysts. It seems that catalytic activity in the WGS reaction is closely related with acid–base properties of the support.

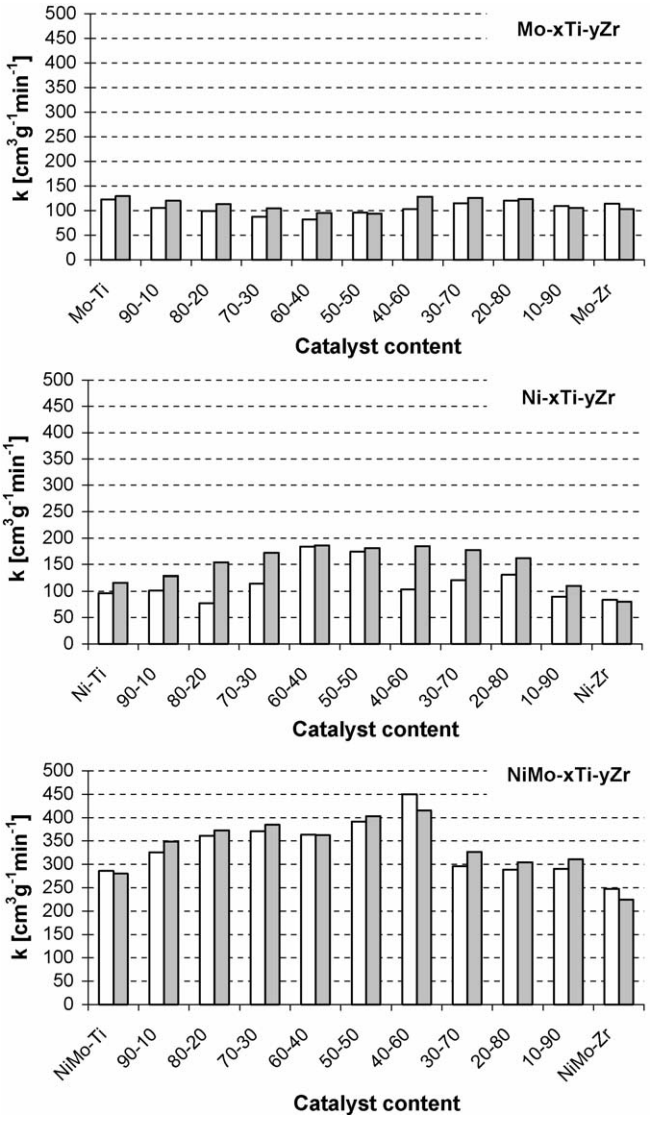

Fig. 5. Catalytic activity of sulfided of Mo, Ni and Ni–Mo catalysts supported on TiO_2–ZrO_2 supports in the WGS reaction after 10 min (white columns) and 120 min (gray columns).

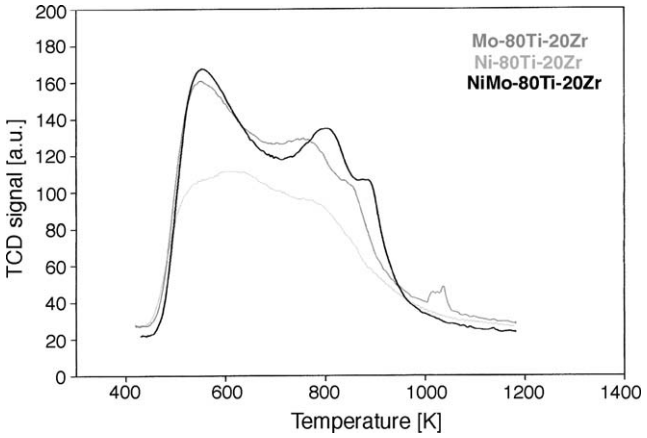

Fig. 6. TPD profiles of ammonia of catalysts supported on 80 wt.% TiO_2–20 wt.% ZrO_2.

The results of acidity measurements (TPD method) show that introduction of Ni, Mo or Ni–Mo onto titania–zirconia supports enhance surface heterogeneity and surface acidity. The example given in Fig. 6 shows characteristic changes in ammonia desorption profiles for the selected catalyst. After deposition of nickel ions the TPD curve of ammonia is practically the same like for pure support (compare Fig. 3). Deposition of molybdenum usually lead to the formation of three maxima on TPD curves, representing at least three acidic centers with different strength. FTIR measurements performed for the oxidized form of catalysts showed that Lewis acid sites (bands at 1440 and 1600 cm^{-1}) are predominant surface acid centers. However, the appearance of weak band at 1540 cm^{-1} after interaction of pyridine with samples containing Mo is indicative for the presence of pyrydinium ions PyH^+. The intensity of this band was the highest for Mo–TiO_2 catalyst. In other cases, the intensity of this band was very weak and decreased with increasing ZrO_2 content in the support composition. In the case of Mo–TiO_2 it is assumed that formation of Brönsted acid sites can be the result of formation of Mo^{4+} surface species linked with OH groups. This way, the oxygen–hydrogen bond is weakened and the increase of proton acidity can be generated. This effect, as well as surface acidity of the sulfided samples, is under investigation and it is mainly studied with TPD of ammonia and selected catalytic reactions [31]. The results presented in Table 2 show the drop of acidity of molybdenum containing samples with increasing content of ZrO_2 in support. This is in contrast to the support itself. Presence of the Mo ions in oxidized forms of WGS catalysts decrease the overall acidity what suggests reorganization of the surface and saturation of Lewis acid sites. On the other hand, the strength of these sites is high, because after desorption of pyridine at 425 K at least half of these acidic centers remain on the catalysts surface.

On the basis of FTIR and TPD experiments the highest acidity was found for equimolar mixture of TiO_2 and ZrO_2 (Table 1). Assuming, that one of the most important steps in the WGS reaction is formation of surface formate, then according to the suggestion of Grenoble and Estadt [29] catalysts with more basic character should promote the decomposition towards H_2 and CO_2. Such assumption finds confirmation in the results presented in Fig. 5 for Mo containing catalysts. Activity of sulfided, Mo-supported catalyst decreases until composition of the support reaches equimolar equilibrium. Since that point acidity become lower and activity increases. Although this not the lowest acidity of the studied supports, it seems that at this point the best proportion of acid–base properties for WGS catalysts was reached. This is additionally confirmed by the results of catalytic activity obtained for supported Ni–Mo–S surface species. The highest activity was found for catalysts supported on 40Ti–60Zr support. One could expect that further decrease of acidity could additionally improve catalytic properties of the studied systems. But decrease of acidity not necessarily always results in increase basicity of the support. Presence of basic sites facilitates reducibility of Mo^{6+} ions towards lower oxidation states [30], simultaneously making easier transformation of oxidized forms to sulfided MoS_2 or Mo–Ni–S structures. Presence of basic sites

Table 2
Surface properties of selected, non-sulfided and sulfided NiMo catalysts

Support/catalyst	BET surface area and pore volume				Amount of chemisorbed NO (mmol g^{-1})	TPR maxima of non-sulfided catalysts (K)
	Non-sulfided		Sulfided			
	$m^2\ g^{-1}$	$cm^3\ g^{-1}$	$m^2\ g^{-1}$	$cm^3\ g^{-1}$		
TiO_2	168	0.33	–	–	–	
Mo–TiO_2	144	0.27	113	0.23	0.16	720, 1030
Ni–TiO_2	142	0.28	125	0.26	0.04	700
NiMo–TiO_2	132	0.25	99	0.22	0.41	650, 1030
60Ti–40Zr	279	0.44	–	–	–	
Mo–60Ti–40Zr	236	0.35	184	0.33	0.17	710, 930, 1040
Ni–60Ti–40Zr	237	0.40	208	0.36	0.07	730
MoNi–60Ti–40Zr	224	0.32	161	0.29	0.46	650, 930, 1030
40Ti–60Zr	269	0.39	–	–	–	
Mo–40Ti–60Zr	234	0.34	180	0.28	0.17	720, 930, 1040
Ni–40Ti–60Zr	236	0.38	207	0.34	0.08	740
MoNi–40Ti–60Zr	222	0.32	158	0.24	0.47	630, 930, 1030
ZrO_2	166	0.19	–	–	–	
Mo–ZrO_2	139	0.17	108	0.16	0.16	700, 980
Ni–ZrO_2	140	0.16	123	0.14	0.04	750, 890
MoNi–ZrO_2	130	0.14	93	0.13	0.39	590, 700, 970

promotes dissociative water decomposition over vacancies localized on MoS_2 and formation of surface species of the oxide–hyrdoxide type which much easier undergo resulfidation in H_2S presence. Introduction of nickel ions onto already supported molybdenum oxide both lowers reduction temperature of molybdenum (see Fig. 7, Table 2) as well as generates active sites on edges and corners of MoS_2 structures.

Temperature programmed reduction (TPR) measurements performed with oxidized forms of nickel and molybdenum containing samples show that introduction of nickel do not cause significant changes in the amount of observed TPR maxima. The only effect is related with decrease of reduction temperature of the first maximum from ~750 to 650 K. The example of typical TPR profiles is shown on Fig. 7. It is very probable that interactions between nickel and molybdenum oxides generate new links of the Ni–Mo–O type. The presence of Ni^{2+} ions influences mobility of Mo^{6+} ions and increases their dispersion. In consequence the shift of the reduction maximum from 760 to 650 K occurs. This maximum assigned to the reduction of Mo^{6+} to Mo^{4+} ions [32,33] is typical for all Ni–Mo systems independently of the support applied. This effect can further influence catalytic properties of the sulfided systems. The lowering of the reduction temperature of Mo^{6+} in the presence of nickel ions can indicate that during sulfidation with H_2/H_2S mixture the process of formation of Mo–S or Ni–Mo–S is much facilitated. This phenomenon provides better dispersion (see Table 2; NO adsorption) of the supported molybdenum ions in the form of MoS_2 or Ni–Mo–S surface species. More discussions related with acidity (measured with TPD of ammonia) and reducibility (TPR) of the studied samples will be published elsewhere [31].

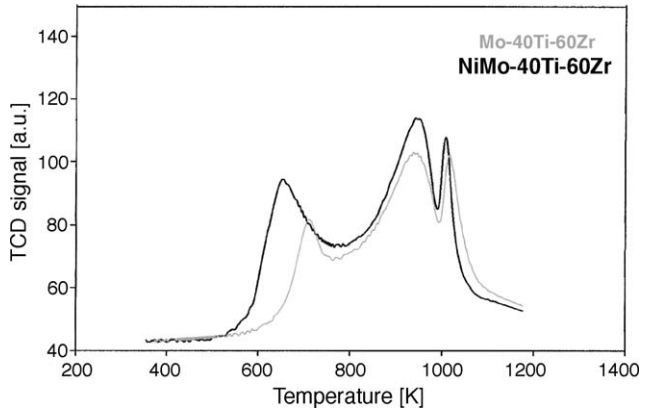

Fig. 7. TPR profiles of catalysts supported on 40 wt.% TiO_2–60 wt.% ZrO_2.

Electronic and structural effects of nickel introduction onto catalytic activity cannot be excluded, as well. Almost doubled dispersion observed for Ni–Mo systems in comparison with those containing only molybdenum supported on analogous supports indicate that structural effects, besides other factors, can influence catalytic behaviour.

4. Conclusions

The Ni–Mo sulfided catalysts supported on TiO_2–ZrO_2 mixed oxides indicate high activity in the WGS reaction with sulfided feed. The choice of the support with high surface area, appropriate ratio of acid–base properties as well as the high dispersion of supported Ni–Mo–S species is responsible for high activity of these catalysts in the WGS reaction.

Introduction of nickel ions onto the molybdenum catalysts causes the increase of dispersion of sulfided molybdenum species independently from support composition. The presence of Ni^{2+} on the surface of molybdenum catalysts decreases temperature of reduction of Mo^{6+} ions and therefore facilitates formation of MoS_2 and Ni–Mo–S species at lower temperature with better dispersion. The highest activity in the WGS reaction was obtained for sulfided catalysts supported on support

composed from 40 wt.% of TiO_2 and 60 wt.% of ZrO_2 and can be related with appropriate ratio of surface acid–base properties of the support.

References

[1] J.N. Armor, Appl. Catal. A: Gen. 176 (1999) 159.
[2] M. Waligórska, M. Łaniecki, Przem. Chem. 84 (2005) 333.
[3] D.S. Newsome, Catal. Rev., Sci. Eng. 21 (1980) 275–318.
[4] K. Kochloefl, in: Ertl, et al. (Eds.), Handbook on Heterogeneous Catalysis, vol. 4, VCH, Weinheim, Berlin, 1997, pp. 1831–1843.
[5] P. Hou, D. Mekker, H. Wise, J. Catal. 80 (1983) 280.
[6] V. Kettman, P. Balgavy, L. Sokol, J. Catal. 112 (1988) 93.
[7] A.A. Andreev, V.J. Kafedjiysky, R.M. Edreva-Kardijeva, Appl. Catal. A 179 (1999) 223.
[8] M. Łaniecki, M. Małecka-Grycz, F. Domka, Appl. Catal. A 196 (2000) 293.
[9] M. Ignacik, M. Łaniecki, in: L. Petrov, et al. (Eds.), Proceed. Ninth Int. Symposium on Heterogeneous Catal., Varna, Bulgaria, Inst. Catalysis BAS, Sofia, 2000, pp. 925–930.
[10] M. Łaniecki, W. Zmierczak, Zeolites 11 (1991) 18.
[11] M. Łaniecki, W. Zmierczak, Stud. Surf. Sci. Catal. 75 (1993) 2569.
[12] M. Łaniecki, Stud. Surf. Sci. Catal. 83 (1994) 363.
[13] G. Martra, Appl. Catal. A: Gen. 200 (2000) 275.
[14] M. Daturi, A. Cremona, F. Milella, G. Busca, E. Vogna, J. Eur. Ceramic Soc. 18 (1998) 1079.
[15] J. Fung, I. Wang, J. Catal. 130 (1991) 577.
[16] K.T. Jung, A.T. Bell, J. Mol. Catal. A: Chem. 163 (2000) 27.
[17] J.C. Wu, C.S. Chung, J. Catal. 87 (1984) 98.
[18] X. Bokhimi, A. Morales, M. Aguilar, J.A. Toledo-Antonio, F. Pedraza, Int. J. Hydrogen Energy 26 (2001) 1279.
[19] O. Ruff, F. Ebert, Z. Anorg. Allg. Chem. 180 (1929) 19.
[20] T. Yamaguchi, Catal. Today 20 (1994) 199.
[21] J.A. Navio, M. Macias, F.J. Marchena, J.M. Campelo, J.M. Marinas, Stud. Surf. Sci. Catal. 75 (1992) 2597.
[22] J. Fung, I. Wang, Appl. Catal. A 166 (1998) 327.
[23] J.C. Wu, C.S. Chung, C.L. Ay, I. Wang, J. Catal. 87 (1984) 98.
[24] J.G. Weissman, E.I. Ko, S. Kaytal, Appl. Catal. A 94 (1993) 45.
[25] J. Fung, I. Wang, Appl. Catal. A: Gen. 166 (1998) 327.
[26] N.K. Ng, J. Phys. Chem. 91 (1987) 2324.
[27] C.V. Caceres, J.L.G. Fierro, J. Lazzaro, A. Lopez-Agudo, J. Soria, J. Catal. 122 (1990) 113.
[28] M.I. Zaki, B. Vielhaber, H. Knözinger, J. Phys. Chem. 90 (1986) 3176.
[29] D.C. Grenoble, M.M. Estadt, J. Catal. 67 (1981) 90.
[30] A. Andreev, R.M. Edreva-Kardijeva, Appl. Catal. A: Gen. 179 (1999) 223.
[31] M. Łaniecki, M. Ignacik, in preparation.
[32] E.C. DeCanio, D.A. Storm, J. Catal. 130 (1991) 653.
[33] E. Payen, S. Kasztelan, J. Grimbolt, J.P. Bonelle, J. Raman Spectrosc. 17 (1986) 233.